Solution Structure and Dynamics of G1TE, a Nonphosphorylated Cyclic Peptide Inhibitor for the Grb2 SH2 Domain

Yuan-Chao Lou,* Feng-Di T. Lung,†,1 Ming-Tao Pai,* Shiou-Ru Tzeng,*
Sue-Yee Wei,* Peter P. Roller,‡ and Jya-Wei Cheng*,1

*Division of Structural Biology and Biomedical Science, Department of Life Science, National Tsing Hua University,
Hsinchu 300, Taiwan, Republic of China; †Department of Nutrition, China Medical College, Taichung 400,
Taiwan, Republic of China; and ‡Laboratory of Medicinal Chemistry, Division of Basic Sciences,
National Cancer Institute, National Institutes of Health, 37/5C-02, Bethesda, Maryland 20892

The solution structure and dynamics of G1TE, a non-phosphorylated cyclic peptide inhibitor for the Grb2 SH2 domain, was determined using two-dimensional NMR and simulated annealing methods. G1TE consists of 10 amino acids and a C-terminal Cys cyclized through its side-chain sulfur atom by a thioether linkage to its N terminus. The results indicate that G1TE assumes a circle-like shape in solution in which all the side chains are protruding outside, and none of the residues are involved in intramolecular hydrogen bonding. The average root-mean-square deviations were found to be 0.41 ± 0.11 Å for the backbone heavy atoms C, Cα, and N, and 1.03 ± 0.14 Å for all heavy atoms in a family of 10 structures. ^{15}N relaxation measurements indicate that G1TE has rather restricted dynamics in the fast time scale within its backbone. However, residues Tyr3, Val6, and Gly7 may be involved in a possible conformational exchange. The structural comparison between G1TE in solution and the BCR-Abl phosphopeptide bound to Grb2 SH2 domain revealed that G1TE may form a larger circle-like binding surface than the BCR-Abl phosphopeptide in the bound form. Also, the restricted backbone dynamics of G1TE may result in a reduced loss of entropy and can compensate for the absence of a phosphate group at the Tyr3 position. These structural and dynamic properties of G1TE may provide a molecular basis for understanding its interactions with the Grb2 SH2 domain. © 1999 Academic Press

The receptor protein tyrosine kinases, when binding to their specific growth factors, dimerize and stimulate their protein kinase activity, which is responsible for reciprocal transphosphorylation of intracellular domains. The Src homology 2 (SH2)[2] domain (~100 amino acids) of intracellular proteins can bind to these tyrosine phosphorylation sites with high affinity. The binding specificity is determined by the residues immediately surrounding the phosphorylated tyrosine (1–3). The SH2 domain of Grb2 binds phosphotyrosyl peptides with the consensus sequence pYXNX within several proteins such as the SHC adapter protein (4, 5), the *erb*B family growth factor receptors (4, 6–9), the FAK morphology-determining protein (10), and the BCR-*abl* cellular oncogenic protein (7). Binding of the Grb2 SH2 domain to the receptors relocates the Grb2 SH3 domain binding proteins, such as Sos, close to the plasma membrane. Sos, which possesses guanine nucleotide exchange activity, then converts the GDP-bound inactive form of Ras to its GTP-bound active form (11–13). Activated Ras triggers the kinase cascade that is essential for cell growth and differentiation. A particularly important role for Grb2 in human

[2] Abbreviations used: SH2, Src homology 2; TFA, trifluoroacetic acid; TPPI, time-proportional phase incrementation; TOCSY, total correlation spectroscopy; DQF-COSY, double-quantum-filtered correlation spectroscopy; NOE, nuclear Overhauser effect; NOESY, nuclear Overhauser effect spectroscopy.

cancer has been proposed for the cells transformed by high levels of *erb*B2 (HER-2 or *neu*) expression (14, 15). Recent studies have indicated that Grb2 function is required for cell transformation by the *neu* and *bcr-abl* oncogenes (16, 17). Thus, the design for specific inhibitors of the Grb2 SH2 domain holds the promise for targeted treatment of breast cancer and other human cancers.

The structure of Grb2 was shown to comprise three distinct domains, with two SH3 domains separated from the SH2 domain by an interlaced junction (18). The crystal structure of the Grb2 SH2 domain in complex with a high-affinity phosphotyrosyl peptide ligand corresponding to the sequence 174–180 of BCR-Abl (KPFpYVNV) has been determined recently (19), and an NMR-based solution structure of an SHC-derived 12-mer phosphopeptide complexed with the same protein was also reported (20). The general folding pattern of the SH2 domain is the same as reported for the full-length Grb2 structure and for the SH2 domains of other proteins. However, substantial differences appear in the conformation of the loops forming the binding site of the target peptide. Specifically, the Trp-121 residue of the EF loop plays a major role in determining the specificity of Grb2-SH2 (19). Recent studies have shown that the phophotyrosyl peptide forms a β-turn-type structure in contrast to all previously reported SH2 binding peptides (19, 20). Subsequently, various inhibitors of the Grb2 SH2 domain were designed based on this structure (21, 22).

Until now, most of the inhibitors designed for the Grb2 SH2 domain have focused on phosphotyrosine-containing peptides and peptidomimetics. However, there are major problems associated with studying such agents in biological media, including their susceptibility to phosphatases and poor cellular uptake. Recently, a series of nonphosphorylated cyclic peptide ligands were discovered for the Grb2 SH2 domain using a phage display library (23). However, these peptides require an internal disulfide bond to maintain the active binding conformation. Subsequently, a redox-stable thioether cyclized peptide analog was developed that showed equipotent Grb2 SH2 domain binding properties (23–25). Since these cyclic peptides do not have phosphotyrosine, they define a new type of SH2 domain binding motif that may advance the design of Grb2 inhibitors. In this paper we report the synthesis and the solution structure of this thioether cyclized nonphosphorylated peptide, G1TE (Fig. 1A), using two-dimensional ^{1}H NMR techniques. We have also synthesized ^{15}N-labeled G1TE to investigate its backbone dynamics using two-dimensional heteronuclear NMR techniques. This structural and dynamics information of G1TE may provide a molecular basis for understand-
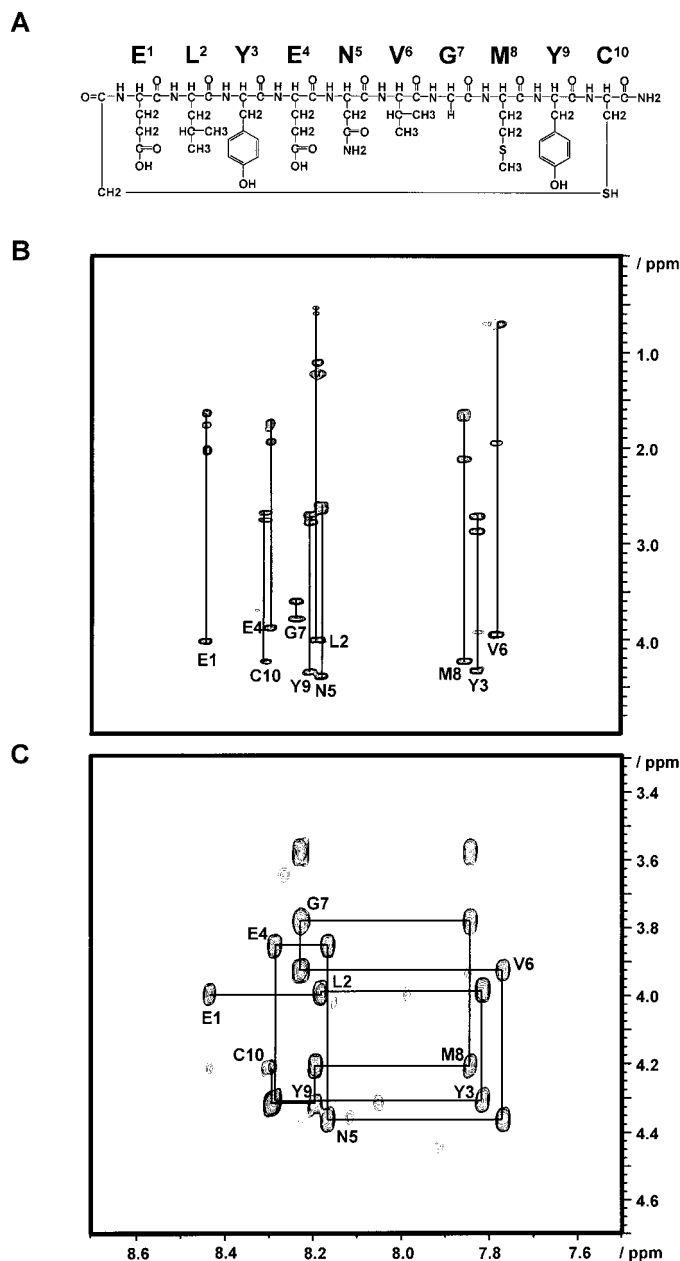

FIG. 1. (A) Chemical structure of G1TE. (B) 600-MHz TOCSY spectrum, recorded at 75-ms mixing time of G1TE at 10°C, showing the NH(F2)-aliphatic(F1) region. (C) NH-C$^{\alpha}$H region of the 600-MHz NOESY spectrum recorded at 250-ms mixing time for G1TE at 10°C. Peaks are labeled at the positions of the NH-C$^{\alpha}$H cross-peaks.

ing the role of G1TE in its interaction with the Grb2 SH2 domain.

MATERIALS AND METHODS

Sample preparations. The targeted peptide was synthesized using Fmoc-based solid-phase synthesis with PAL resin (25). The thioether linkage was carried out by first preparing the N-terminally chloroacetylated derivative of the open chain 10-mer precursor hav-

TABLE I

^{1}H and ^{15}N Chemical Shifts and Temperature Dependence of Amide Proton Resonances
of the G1TE Peptide at 10°C and pH 6.5 in 90%H$_2$O/10%D$_2$O

Residue	$\Delta\delta/\Delta T$ (ppb/K)	Chemical shift (ppm)					
		NH	^{15}N	H$_\alpha$	H$_\beta$	H$_\gamma$	Others
Glu1	4.9	8.45		4.03	1.65/1.77	2.04	C$_\delta$0.54/0.60
Leu2	3.7	8.19	120.6	4.01	1.11/1.24		
Tyr3	6.0	7.83	119.2	4.34	2.88/2.73		
Glu4	5.2	8.30		3.88	1.75/1.81	1.95	
Asn5	5.8	8.19		4.40	2.61/2.67		
Val6	6.8	7.79	117.4	3.96	1.96	0.71	
Gly7	4.8	8.24	111.2	3.61/3.81			
Met8	5.4	7.86		4.24	1.65/1.68	2.13	
Trp9	4.2	8.21	120.8	4.35	2.71/2.78		
Cys10	5.3	8.31		4.25	2.69/2.76		

ing a cysteine located at the C-terminal position, followed by intramolecular displacement of the chloride by the cysteine thiol (26). Removal of the N-terminal Fmoc protecting group was accomplished by gentle stirring with 20% piperidine in dimethylformamide for 20 min at room temperature. The crude peptide was purified by HPLC using a Vydac C$_{18}$ reversed-phase column with two solvent systems of 0.1% TFA/H$_2$O and 0.1% T'FA/acetonitrile. ^{15}N-Labeled G1TE was synthesized using the same procedures with ^{15}N-labeled amino acids at the Leu2, Tyr3, Val6, Gly7, and Tyr9 positions. These peptides were identified by electrospray mass spectroscopy.

NMR spectroscopy. NMR spectra of G1TE were recorded at 600 MHz (Bruker AVANCE-600). The NMR sample was prepared by dissolving 4 mg (3.2 mM) of peptide in 500 μL of 10 mM NaN$_3$, 0.1 mM EDTA, 50 mM K$_3$PO$_4$, 100 mM NaCl buffer containing H$_2$O/D$_2$O (9:1) at pH 3.5. TOCSY with a mixing time of 75 ms and NOESY with mixing times of 70, 150, 250, and 400 ms were carried out with presaturation of water during a relaxation delay of 1.4 s. Data were collected with 256 t_1 increments and 2048 complex data points by a time-proportional phase incrementation (TPPI) method with a sweep width of 6000 Hz. DQF-COSY spectra were collected with 512 t_1 increments and 2048 complex data points. The NMR spectra were processed on a SGI Indigo2 workstation using XWIN-NMR software (Bruker) with the final matrix of 2K $\times$ 1K real data points. A squared sine bell filter shifted by 45° was performed in both dimensions prior to Fourier transformation.

^{15}N *relaxation measurements.* ^{15}N T_1, T_2 and ^{1}H–^{15}N NOE experiments were performed as described (27, 28). The relaxation delays in the T_1 experiments were 0.03, 0.08, 0.15, 0.30, 0.50, 0.75, 1.00, 2.00, 3.00, and 5.00 s, whereas those in the T_2 experiments were 0.004, 0.032, 0.086, 0.151, 0.215, 0.323, 0.539, 0.863, 1.294, and 1.617 s. A recycle delay of 4 s was used for measurements of ^{1}H–^{15}N NOE and a 3-s proton presaturation period was employed for NOE spectra.

The temperature dependence of the amide proton chemical shifts were measured by one-dimensional NMR experiments at 5 to 45°C with a gradual increase of 5°C using a variable temperature probe. The coupling constants ($^3J_{HN\alpha}$) were measured from DQF-COSY spectra by using the method of Kim and Prestegard (29). Interproton distances were computed from NOESY spectra by the distance extrapolation method (30). The side chains of Glu1 and Tyr9 were stereospecifically assigned using a short-mixing-time (15-ms) TOCSY (31). All other side chains of the amino acids in the peptide could not be assigned stereospecifically either due to overlapping of H$_\beta$ cross-peaks or average $^3J_{\alpha\beta}$ coupling constants. Therefore, they were considered as pseudo-atoms during the calculation.

Structure calculation. The structure calculations were carried out with the program X-PLOR 3.851 (Brünger, 1992) on a SGI Indigo2 workstation. Basically, the starting structure was generated using the program Insight II, and then it was cyclized using NOE and thioether constraints by running the *ab inito* simulated annealing protocol, "sa.inp" in X-PLOR 3.851. All force constants, molecular parameters, etc., were set to their default values as in the original sa.inp protocols, with the exception of the time step, which was decreased to 0.001 ps throughout the calculations. Simulated annealing was performed using 6000 steps at 1000 K and 4000 steps by gradually cooling the temperature to 100 K. The structures generated by the SA procedure were refined using SA refinement, "refine.inp." The temperature in refine.inp was set to 1000 K and it was gradually cooled to 100 K in 15000 steps. Finally, these structures were energy-minimized using 300 steps of Powell energy minimization.

The final 50 structures contained distance constraint violations not greater than 0.3 Å and dihedral angle constraint violations not greater than 3°. From these a family of 10 were chosen based on their total energy. An average structure was calculated by averaging the 10 structures, and this average structure was finally refined using the refine.inp protocol as mentioned above.

RESULTS

Resonance assignments and analysis of NMR data. The assignment of all the proton resonances of G1TE was performed using standard NMR procedure (32). Assignments of all proton chemical shifts were accomplished using TOCSY and NOESY spectra, and their chemical shifts are summarized in Table I. The spin systems of Leu2, Val6, and Gly7 were easily identified by their characteristic spin coupling patterns (Fig. 1B). The Tyr3 resonance could be distinguished from that of Tyr9 by its NH–C$_\alpha$H as well as NH–NH connectivity with Leu2 from the NOESY spectrum (Fig. 1C). Similarly, all other residues could be easily assigned from the NOESY spectrum. The interresidual NOEs were all sequential. The absence of long-range NOE between all the protons indicates that the backbone of the cyclic peptide probably forms a circle or loop shape in which all the side chains are protruding outside.
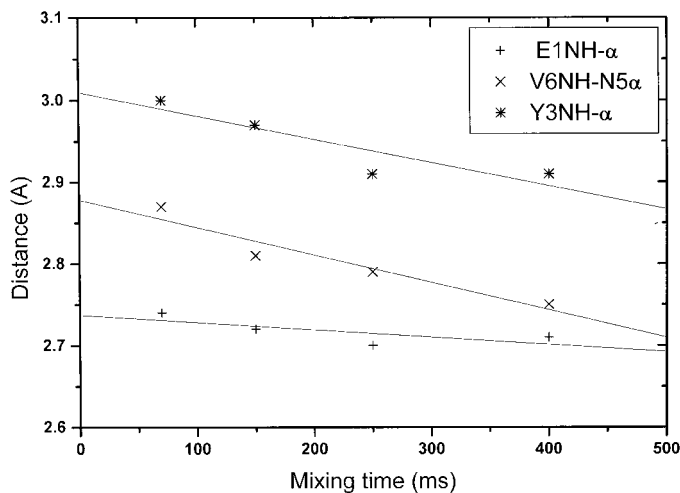
FIG. 2. Time dependence of some NOEs in G1TE measured from the NOESY spectra at four mixing times. The extrapolation of the least-squares fitted lines to zero mixing time yields interproton distances.

TABLE II

Interproton Distances, $d_{\alpha N}(i, i)$ and $d_{\alpha N}(i, i + 1)$, Measured from NOEs Using the Distance Extrapolation Method

Proton pair	Distance (Å)	Proton pair	Distance (Å)
E1NH–E1Hα	2.7	V6NH–V6Hα	3.2
Y3NH–L2Hα	2.6	G7NH–V6Hα	2.5
Y3NH–Y3Hα	3.0	G7NH–G7Hα	2.5
E4NH–E4Hα	2.5	M8NH–G7Hα	2.5
N5NH–E4Hα	2.4	M8NH–M8Hα	2.9
N5NH–N5Hα	2.4	Y9NH–M8Hα	2.6
V6NH–N5Hα	2.9	Y9NH–Y9Hα	2.7

Temperature dependence. The chemical environment of amide protons of G1TE was obtained from the temperature dependence of their chemical shifts. The resonance of a hydrogen-bonded amide proton exhibits smaller downfield chemical shift with increase in temperature compared with one that is exposed to the solvent (33). Normally, an external NH orientation is indicated by an NH signal moving downfield ≥ 4.0 ppb/K with increase in temperature (temperature gradient ≥ 4.0 ppb/K), whereas intramolecular hydrogen bonding is indicated when this value is smaller than 2.0 ppb/K (34). The fact that all the temperature coefficients of G1TE are higher than 2.0 ppb/K (Table I) clearly indicates that no residue is involved in a significant intramolecular hydrogen bonding. This further supports our hypothesis, as mentioned above, that the backbone of the cyclic peptide may form a circular shape.

NMR constraints. NOESY spectra were recorded at 10°C and the NOE intensities of the cross-peaks in each spectrum were calibrated using the isolated-spin-pair approximation, $r_{ij} = r_{ref}(a_{ref}/a_{ij})^{1/6}$, where r_{ij} is the interproton distance to be estimated and a_{ij} is the corresponding 2D NOE cross-peak intensity; r_{ref} and a_{ref} are a known interproton distance and its cross-peak intensity. The average of volume integrals of the geminal interactions between Gly7 Hα1/ Hα2 and Tyr3 Hβ1/Hβ2 were used as reference, and an interproton distance of 1.8 Å was assumed for both. Distance buildup rate was obtained by least-squares fitting of the four measured points (Fig. 2). Extrapolation of the straight line to the ordinate yielded the distance between the respective points. All NOE cross-peaks were used to obtain their interproton distances from the distance extrapolation method. The up-

per and lower bounds of distances for structure calculation were generated by adding ± 0.3 Å to the measured distances lower than 3 Å and by adding ± 0.5 Å to the remaining constraints. The resulting upper bounds of distances $d_{\alpha N}(i, i)$, and $d_{\alpha N}(i, i + 1)$ were lower than 3.2 Å (Table II).

Solution structure of G1TE. The NOE-derived 59 distance constraints and 12 dihedral angle constraints were used for structure calculation by applying the simulated annealing protocol and refine.inp described under Materials and Methods section. After calculation, a family of 10 structures that satisfied the NMR-derived constraints were selected. All of the structures have NOE energies lower than 20 kcal/mol. The structural statistics for the 10 structures are listed in Table III. The resultant structures were superimposed to good convergence (Fig. 3). The average rms deviations calculated versus the mean structure were found to be 0.41 ± 0.11 Å for the backbone heavy atoms C, Cα, and N and 1.03 ± 0.14 Å for all heavy atoms.

Backbone dynamics of G1TE. The ^{15}N chemical shifts for Leu2, Tyr3, Val6, Gly7, and Tyr9 are listed in Table I and their backbone ^{15}N R_1 $(1/T_1)$, R_2 $(1/T_2)$, and ^{15}N–^{1}H NOE values are summarized in Table IV. It should be noted that G1TE has a rather restricted

TABLE III

Structural Statistics for the Family of 10 G1TE Structures

Total no. of restraints	
Interresidual	46
Intraresidual	72
Dihedral angle	12
Atomic rmsd	
Backbone atoms	0.41 ± 0.11
All heavy atoms	1.03 ± 0.14
Deviations from idealized geometry	
Bonds (Å)	0.003 ± 0.001
Angles (deg)	0.307 ± 0.006
Impropers (deg)	0.165 ± 0.013

backbone dynamics on the fast time scale as indicated from the similar R_1 and positive ^{15}N–^1H NOE values (27, 28, 35). However, R_2 values for residues Tyr3, Val6, and Gly7 are quite large, indicating a possible conformational exchange in this region (36, 37).

DISCUSSION

The crystal structure of the Grb2 SH2 domain in complex with the BCR-Abl peptide reveals that this phosphotyrosyl peptide forms a β-turn-type structure due to the Trp121 residue at the EF loop of the Grb2 SH2 domain (19). Based on this structure, various inhibitors of the Grb2 SH2 domain were designed (21, 22). However, in all the cases the "phosphotyrosyl pharmacophore" is very important for binding with the Grb2 SH2 domain and removal of the phosphate group of these peptidomimetics resulted in their loss of binding ability (38).

Recently, it was found that nonphosphorylated cyclic peptide ligands, such as G1TE, can bind with the Grb2 SH2 domain (23). The alanine mutation studies indicated that all amino acids, except Gly7, are essential for activity of G1TE (23). However, there is no sufficient structural information available to explain the nature of binding of G1TE with the Grb2 SH2 domain. In this paper we determined the solution structure and dynamics of G1TE. The backbone of G1TE forms a circular shape in which all the side chains are protruding outside, and no residue is involved in the intramolecular hydrogen bonding. The strong binding of G1TE to the Grb2 SH2 domain, even in the absence of favored electrostatic interactions of the Tyr3 phosphate group, may arise from its correctly positioned circular or loop conformation, which provides it more binding surface compared with the BCR-Abl peptide (Fig. 3). By comparing various analogs of G1TE, it was found that the binding affinity to Grb2 SH2 protein was very much dependent on the ring size of the cyclic peptides (25). Thus G1TE may form a properly folded turn structure that is stabilized by virtue of its cyclized nature,
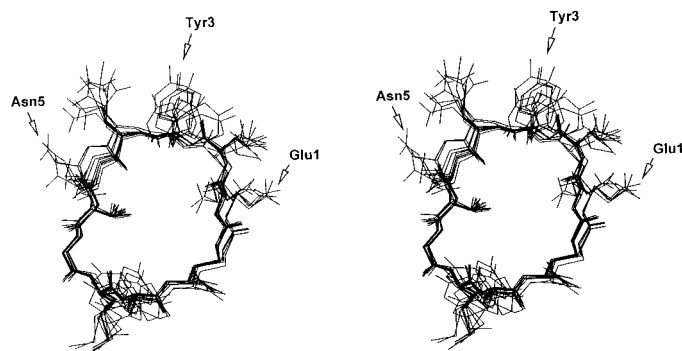
TABLE IV

^{15}N Relaxation Parameters for Leu2, Tyr3, Val6, Gly7, and Tyr9 of G1TE

	R_1 (s^{-1})	R_2 (s^{-1})	NOE
Leu2	1.70 ± 0.01	2.86 ± 0.02	0.36 ± 0.02
Tyr3	1.74 ± 0.01	5.16 ± 0.04	0.37 ± 0.02
Val6	1.60 ± 0.01	4.62 ± 0.04	0.43 ± 0.02
Gly7	1.81 ± 0.02	8.89 ± 0.07	0.40 ± 0.02
Tyr9	1.65 ± 0.01	2.75 ± 0.02	0.32 ± 0.02

thereby resulting in a lower loss of entropy compared with the linear peptides. Indeed, we have found that the backbone dynamics of G1TE is rather restricted based on our ^{15}N relaxation studies. Further structural and dynamic studies on the G1TE/Grb2 SH2 domain complex are needed to clarify these possibilities.

In conclusion we have determined the solution structure and dynamics of the cyclic peptide G1TE using two-dimensional NMR which provides a molecular basis for the design of nonphosphorylated peptidomimetic inhibitors for the Grb2 SH2 domain.

REFERENCES

1. Kuriyan, J., and Cowburn, D. (1993) *Curr. Opin. Struct. Biol.* **3,** 828–837.
2. Pawson, T., and Schlessinger, J. (1993) *Curr. Biol.* **3,** 434–442.
3. Songyang, Z., Shoelson, S. E., Chaudhari, M., Gish, G., Pawson, T., Haser, W. G., King, F., Roberts, T., Ratnofsky, S., Lechleider, R. J., Neel, B. G., Birge, R. B., Fajardo, E. J., Chou, C. M., Hanafusa, H., Schaffhausen, B., and Cantley, L. C. (1993) *Cell* **72,** 767–778.
4. Rozakis-Adcock, M., McGlade, J., Mbamalu, G., Pelicci, G., Daly, R., Li, W., Batzer, A., Thomas, S., Brugge, J., Pelicci, P. G., Schlessinger, J., and Towson, T. (1992) *Nature* **260,** 689–692.
5. Pelicci, G., Lanfrancone, L., Grignani, F., McGlade, J., Cavallo, F., Forni, G., Nicoletti, I., Pawson, T., and Pelicci, P. G. (1992) *Cell* **70,** 93–104.
6. Lowenstein, E. J., Daly, R. J., Batzer, A. G., Li, W., Margolis, B., Lammers, R., Ullrich, A., Skolnik, E. Y., Bar-Sagi, D., and Schlessinger, J. (1992) *Cell* **70,** 431–442.
7. Gale, N. W., Kaplan, S., Lowenstein, E. J., Schlessinger, J., and Bar-Sagi, D. (1993) *Nature* **363,** 88–92.
8. Buday, L., and Downward, J. (1993) *Cell* **73,** 611–620.
9. Egan, S. E., Giddings, B. W., Brooks, M. W., Buday, L., Sizeland, A. M., and Weinberg, R. A. (1993) *Nature* **363,** 45–51.
10. Schlaepfer, D. D., Hanks, S. K., Hunter, T., and Van der Geer, P. (1994) *Nature* **372,** 786–791.
11. Cowburn, D. (1995) *Structure* **3,** 429–430.

FIG. 3. Stereoview of the final 10 structures of G1TE superimposed over the backbone heavy atoms (N, C$^\alpha$, and C).

12. Chardin, P., Cussac, D., Maignan, S., and Ducruix, A. (1995) *FEBS Lett.* **369,** 47–51.

13. Margolis, B. (1994) *Prog. Biophys. Mol. Biol.* **62,** 223–244.

14. Daly, R. J., Binder, M. D., and Sutherland, R. L. (1994) *Oncogene* **9,** 2723–2727.

15. Janes, P. W., Daly, R. J., de Fazio, A., and Sutherland, R. L. (1994) *Oncogene* **9,** 3601–3608.

16. Xie, Y., Pendergast, A. M., and Hung, M. C. (1995) *J. Biol. Chem.* **270,** 30717–30724.

17. Gishizky, M. L., Cortez, D., and Pendergast, A. M. (1995) *Proc. Natl. Acad. Sci. USA* **92,** 10889–10893.

18. Maignan, S., Guilloteau, J., Fromage, N., Arnoux, B., Becquart, J., and Ducruix, A. (1995) *Science* **268,** 291–293.

19. Rahuel, J., Gay, B., Erdmann, D., Strauss, A., Garcia-Echeverria, C., Furet, P., Garavatti, G., Fretz, H., Schoepfer, J., and Grutter, M. G. (1996) *Nature Struct. Biol.* **3,** 586–589.

20. Ogura, K., Tsuchiya, S., Terasawa, H., Yuzawa, S., Hatanaka, H., Mandiyan, V., Schlessinger, J., and Inagaki, F. (1997) *J. Biomol. NMR* **10,** 273–278.

21. Furet, P., Gay, B., Garcia-Echeverria, C., Rahuel, J., Fretz, H., Schoepfer, J., and Caravatti, G. (1997) *J. Med. Chem.* **18,** 3551–3556.

22. Furet, P., Gay, B., Carabatti, G., Garcia-Echeverria, C., Rahuel, J., Schoepfer, J., and Fretz, H. (1998) *J. Med. Chem.* **18,** 3442–3449.

23. Oligino, L., Lung, F. T., Sastry, L., Bigelow, J., Cao, T., Curran, M., Burke, T. R., Wang, S., Krag, D., Roller, P. P., and King, C. R. (1997) *J. Biol. Chem.* **272,** 29046–29052.

24. Lung, F. T., Sastry, L., Wang, S., Lou, B. S., Barchi, J. J., King, C. R., and Roller, P. P. (1999) Proc. 15th Am. Pept. Symp., Vol. 15, 582–583.

25. Lung, F.-D. T., King, R. C., and Roller, P. P. (1999) *Lett. Peptide Sci.* **6,** 45–49.

26. Lindner, W., and Robey, F. A. (1987) *Int. J. Peptide Protein Res.* **30,** 794–800.

27. Cheng, J.-W., Lepre, C. A., Chambers, S., Fulghum, J. R., Thomson, J. A., and Moore, J. M. (1993) *Biochemistry* **32,** 9000–9010.

28. Cheng, J.-W., Lepre, C. A., and Moore, J. M. (1994) *Biochemistry* **33,** 4093–4100.

29. Kim, Y., and Prestegard, J. H. (1989) *J. Magn. Reson.* **84,** 9–13.

30. Baleja, J. D., Moult, J., and Sykes, B. D. (1990) *J. Magn. Reson.* **87,** 375–384.

31. Cai, M., Liu, J., Gong, Y., and Krishnamoorthi, R. (1995) *J. Magn. Reson. Ser. B* **107,** 172–178.

32. Wuthrich, K. (1986) NMR of Proteins and Nucleic Acids, Wiley, New York.

33. Urry, D. W., Ohnishi, M., and Walter, R. (1970) *Proc. Natl. Acad. Sci. USA* **66,** 111–116.

34. Bara, Y. A., Friedrich, A., Kessler, H., and Molter, M. (1978) *Chem. Ber.* **111,** 1045–1057.

35. Lepre, C. A., Cheng, J.-W., and Moore, J. M. (1993) *J. Am. Chem. Soc.* **115,** 4929–4930.

36. Clore, G. M., Szabo, A., Bax, A., Kay, L. E., Driscoll, P. C., and Gronenborn, A. M. (1990) *J. Am. Chem. Soc.* **112,** 4989–4991.

37. Kay, L. E., Torchia, D. A., and Bax, A. (1989) *Biochemistry* **28,** 8972–8979.

38. Yao, Z. J., King, C. R., Cao, T., Kelley, J., Milne, G. W. A., Voigt, J. H., and Burke, T. R., Jr. (1999) *J. Med. Chem.* **42,** 25–35.

39. Brünger, A. T. (1992) A System for X-ray Crystallography and NMR, Yale University, New Haven, CT.